

Local Sustained Delivery of 25-Hydroxyvitamin D₃ for Production of Antimicrobial Peptides

Jiang Jiang · Guojun Chen · Franklin D. Shuler · Chi-Hwa Wang · Jingwei Xie

Received: 10 November 2014 / Accepted: 4 March 2015 / Published online: 14 March 2015
© Springer Science+Business Media New York 2015

ABSTRACT

Purpose This study seeks to develop fiber membranes for local sustained delivery of 25-hydroxyvitamin D₃ to induce the expression and secretion of LL-37 at or near the surgical site, which provides a novel therapeutic approach to minimize the risk of infections.

Methods 25-hydroxyvitamin D₃ loaded poly(L-lactide) (PLA) and poly(ε-caprolactone) (PCL) fibers were produced by electrospinning. The morphology of obtained fibers was characterized using atomic force microscope (AFM) and scanning electron microscope (SEM). 25-hydroxyvitamin D₃ releasing kinetics were quantified by enzyme-linked immunosorbent assay (ELISA) kit. The expression of cathelicidin (hCAP18) and LL-37 was analyzed by immunofluorescence staining and ELISA kit. The antibacterial activity test was conducted by incubating *Pseudomonas aeruginosa* in a monocytes' lysis solution.

Results AFM images suggest that the surface of PCL fibers is smooth, however, the surface of PLA fibers is relatively rough, in particular, after encapsulation of 25-hydroxyvitamin D₃. The duration of 25-hydroxyvitamin D₃ release can last more than 4 weeks for all the tested samples. Plasma treatment can promote the release rate of 25-hydroxyvitamin D₃. Human keratinocytes and monocytes express significantly higher levels of hCAP18/LL-37 after incubation with plasma treated and 25-hydroxyvitamin D₃ loaded PCL fibers than the cells incubated with around ten times amount of free drug. After incubation with this fiber

formulation for 5 days LL-37 in the lysis solutions of U937 cells can effectively kill the bacteria.

Conclusions Plasma treated and 25-hydroxyvitamin D₃ loaded PCL fibers induce significantly higher levels of antimicrobial peptide production in human keratinocytes and monocytes without producing cytotoxicity.

KEY WORDS 25-hydroxyvitamin D₃ · electrospinning · fibers · local sustained delivery · surgical site infection

ABBREVIATIONS

AFM	Atomic force microscope
CFUs	Colony-forming units
DAPI	4',6-diamidino-2-phenylindole
DCM	Dichloromethane
D-MEM	Dulbecco's modified eagle medium
DMF	N, N-dimethylformamide
DMSO	Dimethylsulfoxide
ELISA	Enzyme-linked immunosorbent assay
FBS	Fetal bovine serum
FDA	U.S. Food and Drug Administration
FITC	Fluorescein isothiocyanate
LB	Luria-Bertani
PBS	Phosphate buffer solution

Electronic supplementary material The online version of this article (doi:10.1007/s11095-015-1667-5) contains supplementary material, which is available to authorized users.

J. Jiang · J. Xie (✉)
Department of Surgery and Mary & Dick Holland Regenerative
Medicine Program University of Nebraska Medical
Center, Omaha, Nebraska 68198, USA
e-mail: jingwei.xie@unmc.edu

G. Chen
Bruker Nano Surface Division, Santa Barbara, California 93117, USA

F. D. Shuler
Department of Orthopaedic Surgery, Joan C. Edwards School of
Medicine Marshall University, Huntington, West Virginia 25755, USA

C.-H. Wang
Department of Chemical and Biomolecular Engineering
National University of Singapore, Singapore 117585, Singapore

PCL	Poly(ϵ -caprolactone)
PLA	Poly(L-lactide)
RPMI	Roswell Park Memorial Institute
SEM	Scanning electron microscope

INTRODUCTION

The introduction of antiseptics in the mid-nineteenth century made a significant progress in the prevention of surgical site infections, however, surgical site infections still accounts for up to 38% of all nosocomial infections creating a significant impact on morbidity and mortality with over 290,000 surgical site infections occurring per annum with an estimated inpatient hospital cost of over \$10 billion (1–3). Postsurgical infections lead to increased length of postoperative hospital stay, drastically escalated expenses, higher rates of hospital readmission, and jeopardized health outcomes including a 3% risk of mortality (2,4). Use of traditional antibiotics presents problems of selection and survival of resistant pathogens because of the direct killing mechanism including inhibition of bacterial cell wall synthesis, changing of cytomembrane impermeability, and interference of protein or nucleic acid synthesis (5). Multi-drug resistant nosocomial strains of bacteria such as *Acinetobacter baumannii* have become a major challenge for treatment of surgical site infections and wounds. An ever-rising number of *Acinetobacter baumannii* isolates are exhibiting resistance to essentially all commonly used antibiotics (6–8). The increasing frequency of multidrug-resistant clinical isolates of *Acinetobacter baumannii* in the United States underscores the need for novel approaches to supplement the current antimicrobial treatment regimes used in the prevention of surgical site infections and treatment of wounds (9). To circumvent these problems, new approaches for treatment of surgical site infections with a mode of action different from current anti-infectives are imperatively needed and useful in addressing multiple antibiotic resistant organisms.

Human cathelicidin LL-37 is a small cationic peptide that can act as an antibiotic by disrupting the membrane of microbes (10). LL-37 is derived from an inactive proform (hCAP-18) produced in humans by various types of cells (*e.g.*, keratinocytes, monocytes, neutrophils, macrophages, and epithelial cells) following exposure to active vitamin D (1,25-dihydroxyvitamin D₃) with local production critically dependent on the storage form of vitamin D (25-hydroxyvitamin D₃) (11–14). Direct peptide application and over expression following gene therapy approaches have been used to alter local concentrations of LL-37, but significant issues have developed precluding this direct approach: toxicity to eukaryotic cells, formation of toroidal pore, and risk of unintended and undesired tissue destruction and inflammation in the area of surgical incision (15–19).

The goal of this study was to develop and validate a novel local strategy to effectively minimize the risk of surgical site infections while avoiding direct application of LL-37. Although hydrogels are capable of soft-tissue-like compliance, they can be difficult to suture and are often too weak to support physiologic loads. In addition, it is difficult to encapsulate hydrophobic molecules inside hydrogels. For the sponges, the physical status of hydrophobic drug molecules is usually in crystallized form after encapsulation (20). In order to fulfill our goal, by applying the knowledge of sustained release formulations to design and fabricate fiber-based wound dressings, this study will affect the local delivery of vitamin D based metabolites from biodegradable electrospun fibers. Electrospun fibers can serve as ideal materials for topical drug delivery because of ease of incorporation of drugs, in particular, the hydrophobic molecules inside fibers, ease of control of release profiles by mediating the porosity of fibers and the degradation profiles, hydrophobic drug molecules exhibiting amorphous state and enhancement of solubility of encapsulated hydrophobic drugs (21,22). Compared to traditional wound dressings, fiber-based wound dressings have a number of advantages such as haemostasis, high filtration, semi-permeability, conformability, functional ability and improved cosmetic appearance/scar free (23). However, the current available studies on electrospun fibers for wound dressing are limited to the use of surface modifications or incorporation with chitosan, Ag ions/nanoparticles, ZnO nanoparticles, and antibiotics (24–27). In this work, we hypothesized that electrospun fiber membranes could provide sustained release of 25-hydroxyvitamin D₃. We also hypothesized that 25-hydroxyvitamin D₃ released from fibrous matrices in a sustainable manner could induce the local production of vitamin D dependent antimicrobial peptides (LL-37) and thus provide a novel strategy to minimize the chances of surgical site infections. For the fiber component, we chose PCL and PLA because they are biocompatible and biodegradable and have been approved by the U.S. Food and Drug Administration (FDA) for certain human clinical applications (28,29). Since the critical substrate 25-hydroxyvitamin D₃ was being delivered in this novel approach, the normal host machinery for antimicrobial peptide production was optimized decreasing the risks associated with direct peptide delivery.

MATERIALS AND METHODS

Materials and Reagents

25-hydroxyvitamin D₃ and mouse anti-goat IgG-fluorescein isothiocyanate (FITC) used in the present study was purchased from Santa Cruz biotechnology, Inc. (Dallas, TX, USA). Goat anti-cathelicidin polyclonal antibody was purchased from Abcam (Cambridge, MA, USA). Protease inhibitor cocktail,

PCL (M_w=70~90 kDa) and PLA (M_w=103~259 kDa) were bought from Sigma-Aldrich (St. Louis, MO, USA). Trypsin-EDTA, Dulbecco's Modified Eagle Media and Roswell Park Memorial Institute (RPMI) 1640, 4', 6-diamidino-2-phenylindole (DAPI) were bought from Invitrogen (Grand Island, NY, USA). Triton-X100, M-PER mammalian protein extraction reagent, dichloromethane (DCM), N, N-dimethylformamide (DMF), dimethylsulfoxide (DMSO) and fetal bovine serum (FBS), MicroBCA kit were acquired from Thermo fisher scientific (Waltham, MA, USA). 25-hydroxyvitamin D₃ and LL-37 ELISA kits were purchased from Diagnostika GmbH (Hamburg, Germany) and Hycult biotech (Plymouth Meeting, PA, USA) respectively.

Fabrication of Electrospun Fibers

PCL and PLA fibers with and without 25-hydroxyvitamin D₃ loading were produced using a similar electrospinning setup as reported in our previous studies (30–32). PCL or PLA was dissolved in a solvent mixture consisting of DCM and DMF with a ratio of 4:1(v/v) at a concentration of 10% (PCL) or 4% (PLA) (w/v). The stock solution of 25-hydroxyvitamin D₃ was prepared by dissolving 1 mg 25-hydroxyvitamin D₃ in 1 ml DMSO and was added to the polymer (PCL or PLA) solution with an initial drug loading of 1 mg/g. Polymer solutions were pumped at a flow rate of 0.5 ml/h using a syringe pump while a potential of 12 kV was applied between the spinneret (a 22-gage needle) and a grounded collector located 12 cm apart from the spinneret. A rotating drum was used to collect membranes composed of random fibers with a rotating speed less than 100 rpm. The fiber mats were then treated with air plasma using plasma cleaner (PDC-32G, Harrick Plasma, Ithaca, NY) for 8 min at a medium setting. All the fiber samples were treated by air plasma and sterilized by γ radiation at a dose of 15 kGy prior to use for cell culture.

Morphological Characterization

The morphology and diameter of fiber samples were characterized by a SEM (FEI, Quanta 200, Oregon, USA) and an AFM (Bruker surface metrology division, Goleta, USA). To avoid charging, polymeric fiber samples were fixed on a metallic stud with double-sided conductive tape and coated with platinum for 4 min in vacuum at a current intensity of 10 mA using a sputter coater. SEM images were acquired at an accelerating voltage of 30 kV. The AFM images were obtained in ScanAsyst (peak force) mode by scanning the fibers deposited on the cover glass surface under ambient conditions using a Bruker Catalyst with a NanoScope V Controller. Sharp silicon probes (ScanAsyst air, k ~0.4 N/m, Bruker) were used to collect the images with the parameter settings as below: 512×512 pixels resolution, typical scanning rate 1.5 Hz.

The brightness of features in captured topographic images increases as a function of height of the samples.

In Vitro Release and Encapsulation Efficiency

In vitro release of 25-hydroxyvitamin D₃ from the fibers was evaluated by immersing 10 mg fiber samples in the 10 ml PBS solution at 37°C. The supernatants were collected at each time point and replaced by fresh PBS solutions. Drug loading and encapsulation efficiency were determined by the following procedures. Ten mg fiber samples were dissolved in 0.2 ml glacial acetic acid. The 25-hydroxyvitamin D₃ concentrations of all collected samples were determined by 25-hydroxyvitamin D₃ ELISA kit according to the manufacturer's instructions.

Cell Culture and Treatments

Human keratinocyte cell line (HaCat) and monocyte cell line (U937) were cultured in D-MEM with 10% FBS and RPMI-1640 media with 10% FBS respectively. The cultures were maintained at 37°C under 95% air and 5% CO₂ until reaching 80% confluence. The subconfluent HaCat cells were dissociated with a 0.05% trypsin-EDTA and re-suspended in a fresh complete media. U937 cells were precipitated by 300 g centrifugation and then re-suspended in a fresh complete media. The single HaCat cell suspensions were created by gently pipetting up and down HaCat cell aggregates and then placed in 6-cm culture dishes and incubated for 1 day. At the beginning of experiments, 5.0×10^5 , 2.0×10^5 and 1.0×10^5 cells were seeded in the culture dishes for 1-day, 3-day, and 5-day treatments, respectively. The media was then replaced by D-MEM (Ctr), D-MEM containing 0.52% DMSO, D-MEM containing 5.0×10^{-7} M 25-hydroxyvitamin D₃, D-MEM containing 5.0×10^{-6} M 25-hydroxyvitamin D₃, D-MEM containing 1 mg/ml pristine PCL fibers, and D-MEM containing 1 mg/ml 25-hydroxyvitamin D₃ loaded PCL fibers and incubated for 1, 3, and 5 days. Of note, 5.0×10^{-6} M 25-hydroxyvitamin D₃ was chosen as a free drug control due to cytotoxicity in OKF6-TERT2 cells (33). The single U937 cell suspension was placed in 6-cm culture dishes. Then, the cultures were incubated with RPMI-1640 (Ctr), RPMI-1640 containing 0.52% DMSO, RPMI-1640 containing 1 mg/ml pristine PCL fibers, RPMI-1640 containing 5.0×10^{-7} M 25-hydroxyvitamin D₃, RPMI-1640 containing 5.0×10^{-6} M 25-hydroxyvitamin D₃, and RPMI-1640 containing 1 mg/ml 25-hydroxyvitamin D₃ loaded PCL fibers for 1, 3, and 5 days.

Cell Proliferation

HaCat cells and U937 cells were seeded in 24-well plates. Each well contains 2.5×10^4 cells and 1 ml culture media (D-

MEM for HaCat and RPMI-1640 for U937). The cells were treated following the procedure described in the section of cell culture and treatments. The subconfluent HaCat cells were harvested at day 1, 3 and 5 with 0.05% trypsin-EDTA solution and re-suspended in fresh complete media. U937 cells were re-suspended by gently pipetting up and down. The cell density was calculated based on the cell counting.

Immunofluorescence Assay

After treatments with different formulations, the cells were rinsed with PBS twice and fixed with 4% paraformaldehyde for 30 min at 37°C followed by incubation with TNBS (0.05% Triton-X100, 2% FBS in pH 7.2 PBS) for 30 min at room temperature prior to immunostaining. Goat anti-cathelicidin polyclonal antibody (1:200) was incubated to label intercellular cathelicidin at 4°C for overnight. Mouse anti-goat IgG-FITC antibody (1:100) was incubated for 2 h after removal of primary antibody and wash with TNBS for three times. Then, the secondary antibody was removed and washed by TNBS for three times. Nuclei were counterstained with 10 μ M DAPI in blue. Images were taken with a digital camera (Carl Zeiss). The exposure time for taking images for HaCat and U937 cells was fixed at 400 ms and 40 ms, respectively.

Quantification of LL-37

Single cell suspensions of both HaCat and U937 were seeded in 6-cm culture dishes. At the beginning of experiments, 5.0×10^5 , 2.0×10^5 and 1.0×10^5 cells were seeded in the culture dishes for 1-day, 3-day, and 5-day treatments, respectively. Cells were treated with different formulations as described above and harvested at each time point. The subconfluent HaCat cells and U937 cell suspensions were washed with PBS twice. Subsequently, 300 μ l of the M-PER mammalian protein extraction reagent with 0.1% protease inhibitor cocktail was added to the extraction reagent. They were agitated for 20 min and lysate was collected and transferred to a 1.5-ml microcentrifuge tube. The samples were centrifuged at 14,000 g for 40 min at 4°C to pelletize the cell debris and the supernatant was transferred to a new tube for analysis. Total protein concentration was tested by MicroBCA kit before ELISA test. Concentrations of LL-37 in cell lysate were determined by LL-37 ELISA assay kit based on the manufacturer's instructions.

Bacteria Culture and Colony Forming Unit Test

U937 cells were treated and harvested based on the same protocol in the section of quantification of LL-37. The cell lysis solutions were collected and total protein concentrations were quantified as mentioned above. Then, all the cell lysis solutions were diluted to 1 mg/ml of total protein in PBS. To examine the effect of LL-37 in the cell lysis solution on killing Gram-negative

bacteria, *Pseudomonas aeruginosa* were cultured in liquid Luria-Bertani (LB) medium and subsequently the bacteria were diluted to approximately 10^4 CFUs per microliter in PBS. One hundred μ l of bacteria solution was mixed with 100 μ l of the cell lysis solution and cultured at 37°C for 1 h. Then the culture was placed on a LB agar plate. With additional incubation for 12 h at 37°C, the number of colonies was counted. The counts were repeated with three LB agar plates and averaged.

Statistical Analysis

Three replicates were tested for each data point. The statistical analysis was performed on the means of the data obtained from at least three independent experiments. All the results were presented as means and the significance was assessed using student's *t*-test. *p* values of 0.05 or less among the groups were considered to be significant and very significant.

RESULTS

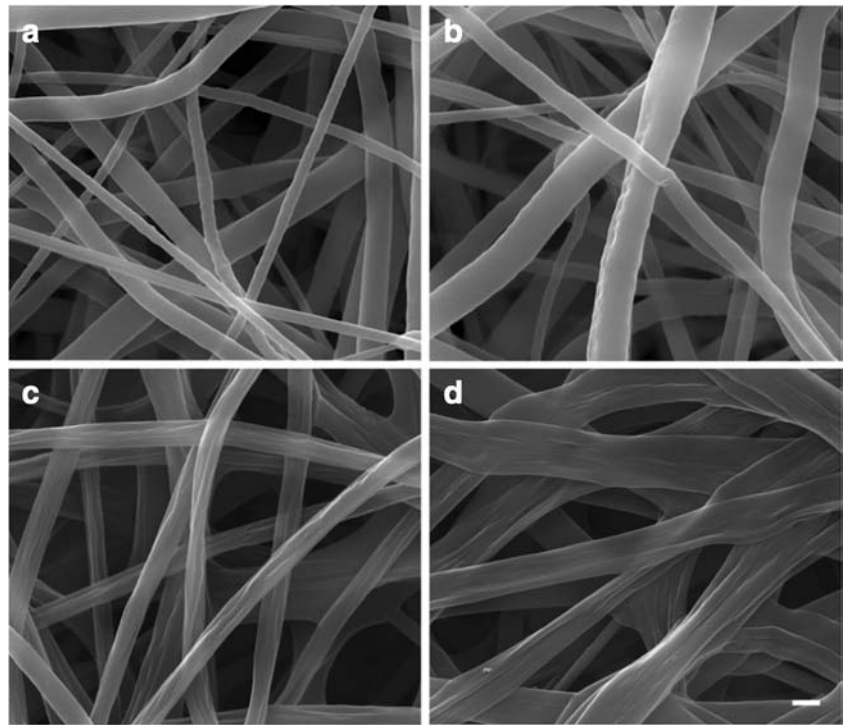
Electrospinning Fiber Characterization

In this work, we chose PCL and PLA as model materials because they are biocompatible and biodegradable polymers and have been approved by FDA for certain human clinical applications. 25-hydroxyvitamin D₃ loaded PCL fibers and 25-hydroxyvitamin D₃ loaded PLA fibers were first fabricated by electrospinning and then treated with air plasma. We first characterize the morphology of fibers using SEM. Figure 1a-d shows SEM images of the morphology of PCL fibers, 25-hydroxyvitamin D₃ loaded PCL fibers, PLA fibers and 25-hydroxyvitamin D₃ loaded PLA. The diameters of PCL fibers, 25-hydroxyvitamin D₃ loaded PCL fibers, PLA fibers and 25-hydroxyvitamin D₃ loaded PLA fibers were 633 ± 296 , 906 ± 446 , 708 ± 156 , and 1204 ± 397 nm. The surface of PCL fibers was smooth and remained almost the same after encapsulation of 25-hydroxyvitamin D₃. In contrast, PLA fibers showed some wrinkles on the surface and more wrinkles was observed on the surface after encapsulation. In addition, the PCL and 25-hydroxyvitamin D₃ loaded PCL fibers were in cylindrical shape while PLA and 25-hydroxyvitamin D₃ loaded PLA fibers shaped like a ribbon. We further characterize the morphology of fibers using AFM shown in Fig. 2. It is seen that the surface of PCL fibers was smooth and similar to that of 25-hydroxyvitamin D₃ loaded PCL fibers. However, the surface of 25-hydroxyvitamin D₃ loaded PLA fibers seemed rougher than PLA fibers.

Drug Releasing Kinetics

We then examined the release kinetics of 25-hydroxyvitamin D₃ from fiber formulations developed using 25-

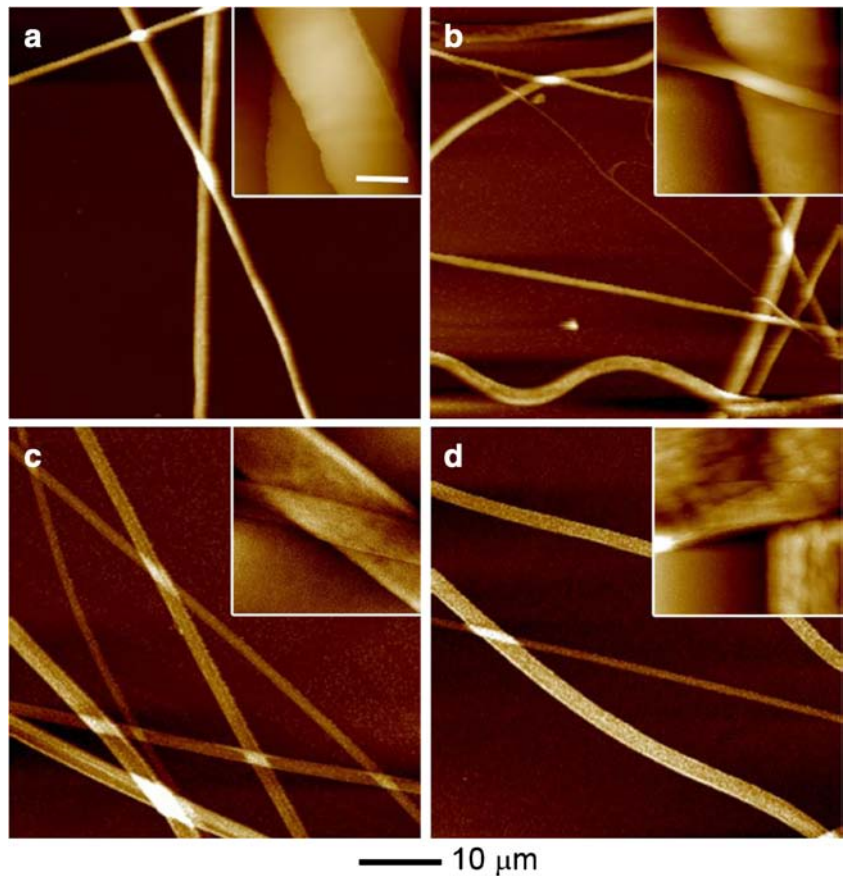
Fig. 1 Morphology characterization. SEM images of (a) PCL fibers, (b) 25-hydroxyvitamin D₃ loaded PCL fibers, (c) PLA fibers and (d) 25-hydroxyvitamin D₃ loaded PLA fibers. The scale bar is 1 μ m for all the panels.



hydroxyvitamin D₃ ELISA kit. The initial drug loading was 1%. The drug loading and encapsulation efficiency for 25-

hydroxyvitamin D₃ loaded PCL were 0.76% and $76 \pm 7.4\%$ while the corresponding values for 25-hydroxyvitamin D₃

Fig. 2 Morphology and surface characterization. AFM images of (a) PCL fibers, (b) 25-hydroxyvitamin D₃ loaded PCL fibers, (c) PLA fibers and (d) 25-hydroxyvitamin D₃ loaded PLA fibers. The scale bar is 1 μ m for all the insets.



loaded PLA fibers were 0.90% and $90 \pm 5.4\%$. Figure 3 shows the *in vitro* release profiles of raw fiber formulations (25-hydroxyvitamin D₃ loaded PCL, 25-hydroxyvitamin D₃ loaded PLA) and plasma-treated and 25-hydroxyvitamin D₃ loaded fiber formulations and plasma-treated and 25-hydroxyvitamin D₃ loaded PLA fiber formulations. Figure 3 shows the cumulative percentage of released 25-hydroxyvitamin D₃ from plasma treated and 25-hydroxyvitamin D₃ loaded PLA fibers was around 5% higher than that from plasma treated and 25-hydroxyvitamin D₃ loaded PCL fibers. Correspondingly, plasma-treated fibers samples showed a similar trend. Around 55% and 49% of 25-hydroxyvitamin D₃ were released from plasma treated and 25-hydroxyvitamin D₃ loaded PLA and plasma treated and 25-hydroxyvitamin D₃ loaded PCL fiber samples after incubation for 28 days. By contrast, only 32% and 23% of 25-hydroxyvitamin D₃ were released from untreated 25-hydroxyvitamin D₃ loaded PLA and 25-hydroxyvitamin D₃ loaded PCL fiber samples within the same incubation time.

Cell Proliferation

Before proceeding to investigate the capability of fiber formulations in inducing the antimicrobial peptide production, we tested the *in vitro* cytotoxicity of various formulations using HaCat cells (human keratinocyte cell line) and U937 cells (leukemic monocyte lymphoma cell line) (Fig. 4). Both types of cells are present during the wound healing process. According to 25-hydroxyvitamin D₃ release profiles, cumulatively released 25-hydroxyvitamin D₃ from 1 mg plasma treated and 25-hydroxyvitamin D₃ loaded PCL fibers was approximately 190

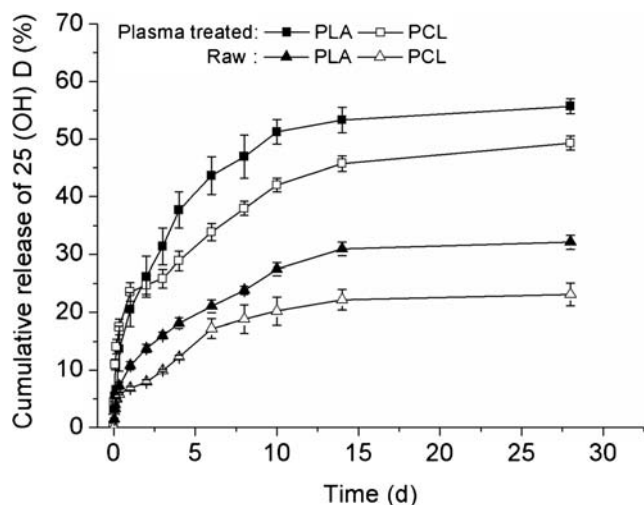


Fig. 3 Release profiles of 25-hydroxyvitamin D₃ from various fiber samples. Solid square (■): 25-hydroxyvitamin D₃ loaded and air plasma treated PLA fibers. Open square (□): 25-hydroxyvitamin D₃ loaded and air plasma treated PCL fibers. Solid triangle (▲): 25-hydroxyvitamin D₃ loaded PLA fibers. Open triangle (△): 25-hydroxyvitamin D₃ loaded PCL fibers. Each data point represents arithmetic mean \pm SD values from three samples.

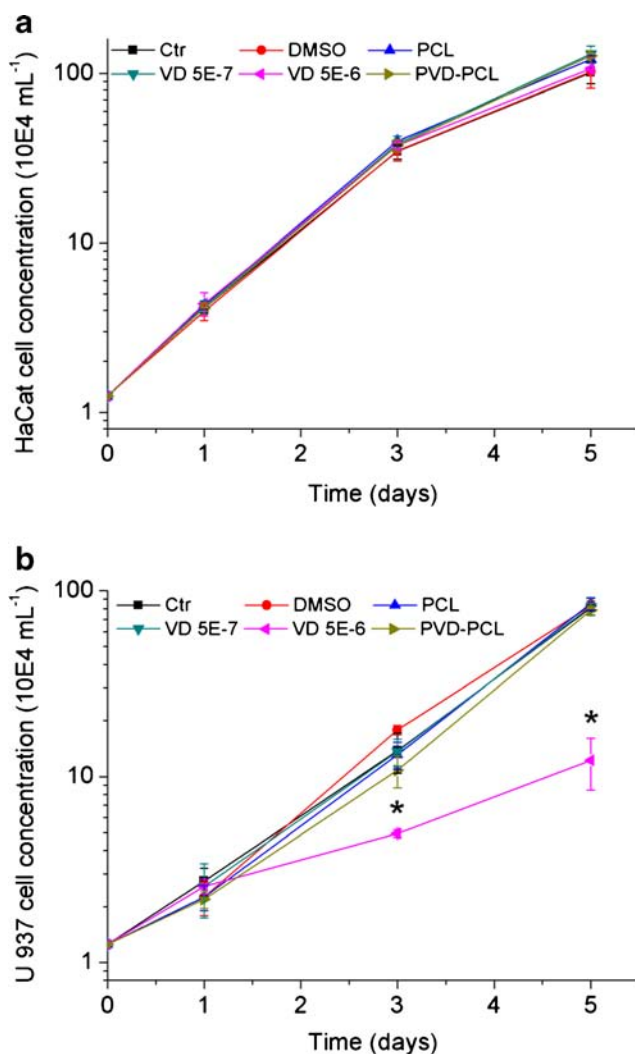


Fig. 4 Cytotoxicity of various formulations. HaCat (a) and U937 (b) cell proliferation after treatment with 1 mg/ml PCL fibers, 0.52% DMSO, 5.0×10^{-7} M 25-hydroxyvitamin D₃, 5.0×10^{-6} M 25-hydroxyvitamin D₃, and 1 mg/ml plasma treated 25-hydroxyvitamin D₃ loaded PCL fibers (containing 5.0×10^{-7} M 25-hydroxyvitamin D₃ equivalent amount based on the calculations from release profiles in the first 3 days) for 1, 3 and 5 days. Each data point represents arithmetic mean \pm SD values from four samples. Statistical significance was calculated by student's *t*-test (**p* < 0.05).

and 230 ng in the first 3 and 5 days, respectively. Therefore, the equivalent concentration of 25-hydroxyvitamin D₃ for 1 mg plasma treated and 25-hydroxyvitamin D₃ loaded PCL fibers in 1 ml media in the first 3 days was $\sim 5.0 \times 10^{-7}$ M. The treatment of 5.0×10^{-7} M 25-hydroxyvitamin D₃ free drug was conducted as a control. The cells treated with 5.0×10^{-6} M 25-hydroxyvitamin D₃ free drug around ten times the concentration of 25-hydroxyvitamin D₃ in the control group was used as an additional toxicity control. Since 1 mg/ml 25-hydroxyvitamin D₃ stock solution was prepared in DMSO, 0.52% DMSO (v/v) was added into complete culture media as a solvent control group. Air plasma treated PCL fibers without drug loading was employed as another control group. Figure 4a shows the change of cell concentrations along with

incubation times after treatment with different formulations. There were no significant differences of HaCat concentration/proliferation after treatment with various experimental groups at each time point, suggesting no evident cytotoxic effect on HaCat cells. However a slight decrease in the proliferation rate was found for all experimental groups after 3 days' incubation, which could be due to the exhaustion of nutrients in the culture media. In contrast, the same treatments on U937 cells showed one notable difference: the proliferation rate of U937 cells reduced dramatically after treatment of 5.0×10^{-6} M 25-hydroxyvitamin D₃ for 3 and 5 days, exhibiting its cytotoxic effects (Fig. 4b). Except for 5.0×10^{-6} M 25-hydroxyvitamin D₃ all other treatment groups showed marginal effects on the proliferation/concentration of U937 cells, indicating no cytotoxicity to the cells.

Expression of hCAP 18

We subsequently pursued the capability of various formulations in inducing the expression of cathelicidin in HaCat cells and U937 cells (Fig. 5). We chose polyclonal of anti-

cathelicidin antibody and FITC conjugated secondary antibody to perform immunofluorescence staining and qualitatively examine the effects of different formulations on the cathelicidin expression. Both the full length and cleaved C terminus of hCAP18 were labeled. We obtained the positive staining of hCAP 18 in HaCat cells after 3 days' treatment of 5.0×10^{-6} M 25-hydroxyvitamin D₃ or incubation with plasma treated and 25-hydroxyvitamin D₃ loaded PCL fibers (Fig. 5a). With increasing the incubation time from 1 day to 3 days to 5 days, the green fluorescence intensity of cells obviously increased when treated with 5.0×10^{-6} M 25-hydroxyvitamin D₃ or plasma treated and 25-hydroxyvitamin D₃ loaded PCL fibers containing $\sim 5.0 \times 10^{-7}$ M 25-hydroxyvitamin D₃ (equivalent amount based on the calculations from release profiles in the first 3 days). Additionally, HaCat cells treated with 5.0×10^{-7} M 25-hydroxy vitamin D₃, DMSO and pristine PCL fibers showed the negative staining at all time points. DMSO and pristine PCL fibers showed no capability in inducing hCAP 18 expressions in HaCat cells. It is interesting to note that

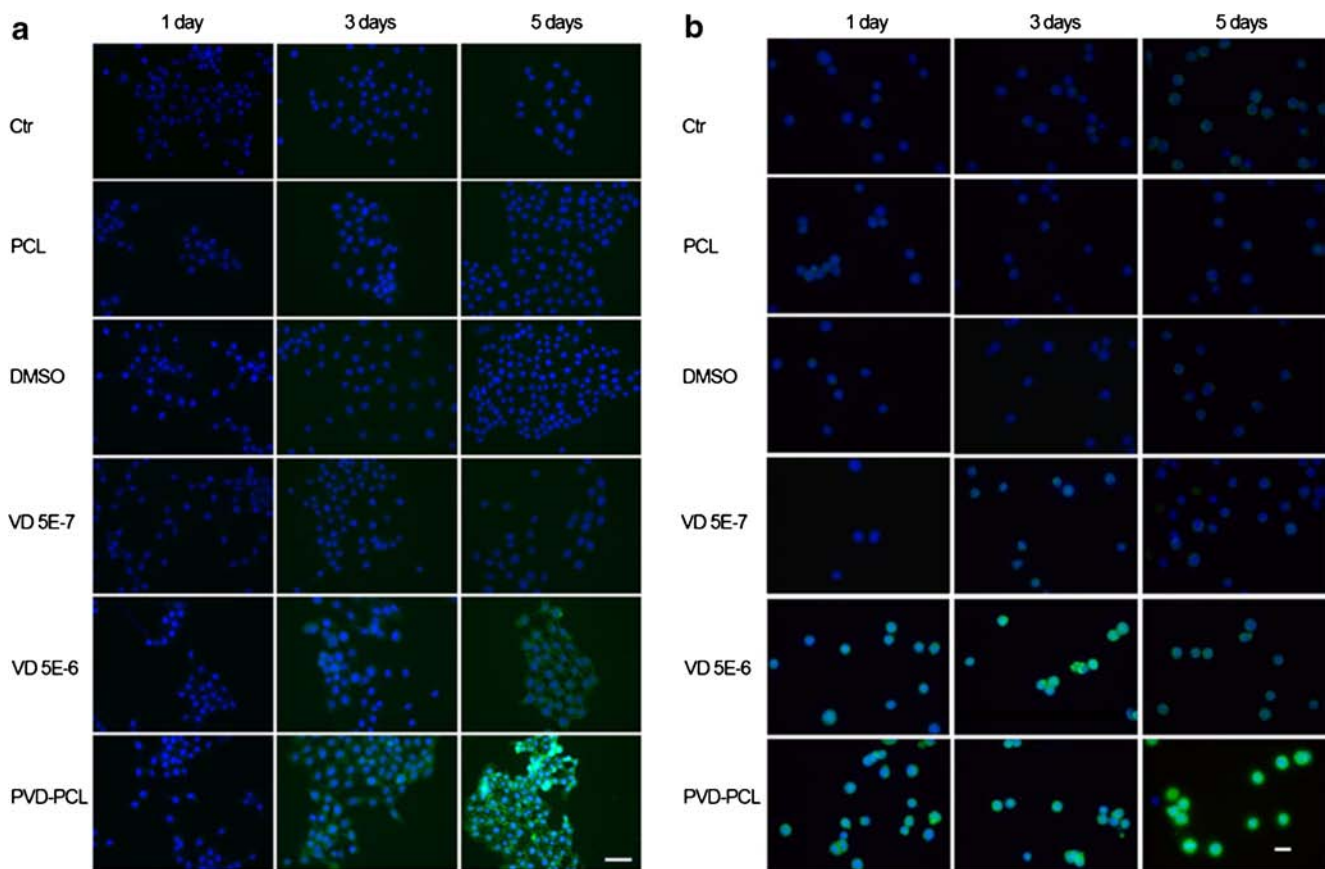


Fig. 5 Cathelicidin expression of HaCat (a) and U937 (b) cells after treatment with different formulations. Fluorescence microscopy images illustrate the cathelicidin expression of HaCat and U937 cells which were incubated in the presence of pristine 1 mg/ml PCL fibers, 0.52% DMSO, 5.0×10^{-7} M 25-hydroxy vitamin D₃, 5.0×10^{-6} M 25-hydroxyvitamin D₃ and 1 mg/ml plasma treated and 25-hydroxyvitamin D₃ loaded PCL fibers (containing 5.0×10^{-7} M 25-hydroxyvitamin D₃ equivalent amount based on the calculations from release profiles in the first 3 days) for 1, 3 and 5 days. The expressed cathelicidin of cultured cells were stained with rabbit anti-cathelicidin antibody and mouse anti-rabbit FITC secondary antibody in green and the nuclei were counterstained with DAPI in blue. The scale bar is 20 μ m.

the 5.0×10^{-7} M 25-hydroxyvitamin D₃ control did not demonstrate hCAP 18 expression.

The same experiments were also conducted using U937 cells (Fig. 5b). Similarly, U937 cells were treated with pristine PCL fibers, DMSO or 5.0×10^{-7} M 25-hydroxyvitamin D₃ showed negative staining of cathelicidin at each time point. By contrast, U937 cells exhibited evident expression of hCAP 18 after 1 day's treatment of 5.0×10^{-6} M 25-hydroxyvitamin D₃ or plasma treated and 25-hydroxyvitamin D₃ loaded PCL fibers containing $\sim 5.0 \times 10^{-7}$ M 25-hydroxyvitamin D₃ (equivalent amount based on the calculations from release profiles in the first 3 days). With increasing incubation time, the fluorescence intensity of U937 cells increased after treatment of 5.0×10^{-6} M 25-hydroxyvitamin D₃ while maintained the similar level when treated with plasma treated and 25-hydroxyvitamin D₃ loaded PCL fibers for 3 days. Intriguingly, the fluorescence intensity (expression level of hCAP 18) of U937 cells decreased after treatment of 5.0×10^{-6} M 25-hydroxyvitamin D₃ from day 3 to day 5, however, the fluorescence intensity (expression level of hCAP 18) of U937 cells sharply increased when treated with plasma treated and 25-hydroxyvitamin D₃ loaded PCL fibers within the same culture period. The cell proliferation assays demonstrated a decrease in cell concentration on days 3 and 5 for the U937 cells treated with 5.0×10^{-6} M 25-hydroxyvitamin D₃.

LL 37 Production

We further quantitatively investigated the production of antimicrobial peptide from HaCat cells and U937 cells after induction of different formulations using LL-37 ELISA kit (Fig. 6). It is seen that the LL-37 production in both HaCat cells and U937 cells was significantly higher when incubated with plasma treated and 25-hydroxyvitamin D₃ loaded PCL fibers than the free drug for 3 and 5 days (Fig. 6). The amount of LL-37 produced from U937 cells increased when treated with 5.0×10^{-6} M 25-hydroxyvitamin D₃ for 3 days and then decreased sharply after 5 days' incubation. This result was in line with the data of hCAP18 expression. Importantly, both HaCat and U937 cells were treated with plasma treated and 25-hydroxyvitamin D₃ loaded PCL fibers had a stable production of high amounts of LL-37. Most interestingly, the cells treated with plasma treated and 25-hydroxyvitamin D₃ loaded PCL fibers containing $\sim 5.0 \times 10^{-7}$ M 25-hydroxyvitamin D₃ (equivalent amount based on the calculations from release profiles in the first 3 days) can produce higher amount of LL-37 than the cells treated with 5.0×10^{-6} M 25-hydroxyvitamin D₃ – 10.3 and 8.3 times concentrations of plasma treated and 25-hydroxyvitamin D₃ loaded PCL fiber group after incubation for 3 and 5 days consistent with the results from cell proliferation and immunofluorescent assays. In addition, it is worth noting that U937 cells can produce a 10-fold larger

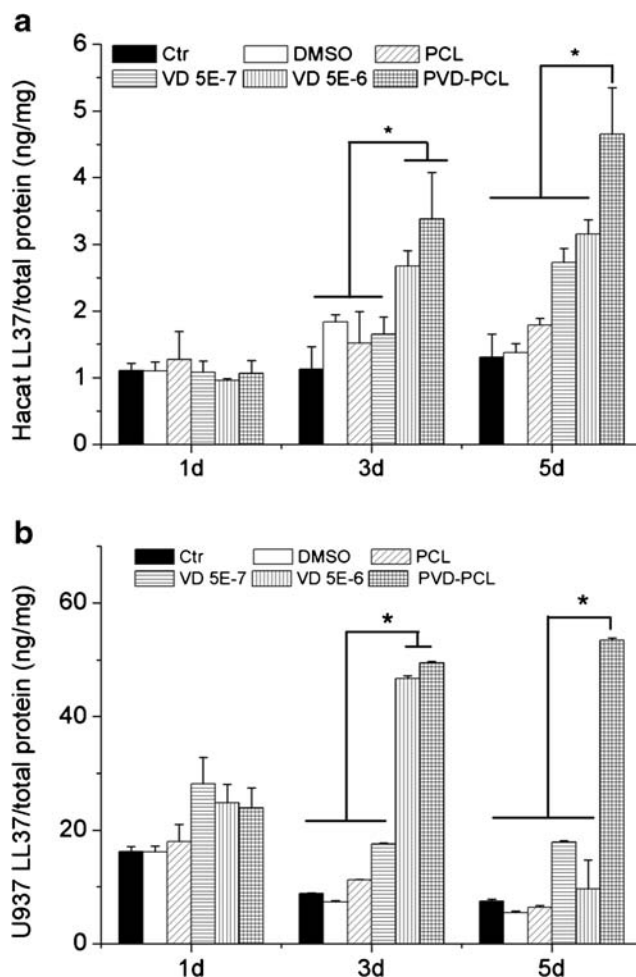


Fig. 6 Quantification of LL37 expressed in HaCat (a) and U937 (b) cells after treatment with different formulations. Cells were incubated in the presence of 1 mg/ml pristine PCL fibers, 0.52% DMSO, 5.0×10^{-7} M 25-hydroxyvitamin D₃, 5.0×10^{-6} M 25-hydroxyvitamin D₃, and 1 mg/ml plasma treated and 25-hydroxyvitamin D₃ loaded PCL fibers (containing 5.0×10^{-7} M 25-hydroxyvitamin D₃ equivalent amount based on the calculations from release profiles in the first 3 days) for 1, 3 and 5 days. Each data point represents arithmetic mean \pm SD values from three samples. Statistical significance was evaluated by student's *t*-test (**p* < 0.05).

amount of LL-37 than HaCat cells under the same testing conditions.

Antibacterial Activity

We also demonstrated antibacterial activity through co-incubation of bacteria and U937 lysis solutions. Bacteria were incubated with cell lysis solutions and CFUs were counted on agar plates. The numbers of CFUs showed no significant difference between the lysis solutions of U937 cells that were treated with different formulations for 1 and 3 days. In contrast, the lysis solutions of cells which were treated with 5.0×10^{-6} M 25-hydroxyvitamin D₃ and plasma treated and 25-hydroxyvitamin D₃ loaded PCL fibers for 5 days showed significantly lower numbers of CFUs than other treatment groups (Fig. 7).

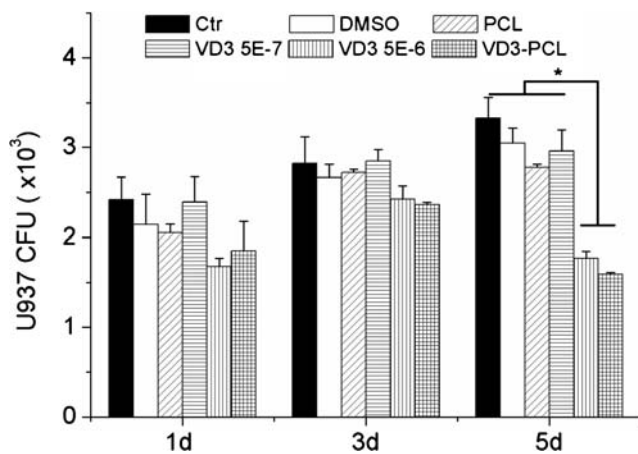


Fig. 7 Quantification of *pseudomonas aeruginosa* CFUs treated by U937 lysis solutions. U937 were incubated in the presence of 1 mg/ml pristine PCL fibers, 0.52% DMSO, 5.0×10^{-7} M 25-hydroxyvitamin D₃, 5.0×10^{-6} M 25-hydroxyvitamin D₃, and 1 mg/ml plasma treated and 25-hydroxyvitamin D₃ loaded PCL fibers (containing 5.0×10^{-7} M 25-hydroxyvitamin D₃ equivalent amount based on the calculations from release profiles in the first 3 days) for 1, 3 and 5 days. Bacteria were incubated with cell lysis solutions and CFUs were counted on agar plates. Each data point represents arithmetic mean \pm SD values from three samples. Statistical significance was evaluated by student's *t*-test (* $p < 0.05$).

DISCUSSION

Surgical site infections continue to represent a significant portion of healthcare-associated infections (2). Antibiotic resistance in common pathogens reinforces the need to minimize surgical site infections (34). Recent studies showed the synthesis of active 1,25-hydroxyvitamin D₃ occurred in numerous extrarenal sites in cells such as keratinocytes, epithelia cells, neutrophils, monocytes and macrophages which express CYP27B1 and vitamin D receptor. The synthesized 1,25-hydroxyvitamin D₃ bound to vitamin D receptor acting as a transcription factor leading to induction of hCAP 18 (11–14,35–37). In its nascent form, hCAP 18 is inactive. Upon cleavage by proteinase 3, LL-37 is generated (38). Therefore, LL-37 can be derived from an inactive form (hCAP-18) produced in humans by various type of cells following exposure to active 1,25-hydroxyvitamin D₃ with local production critically dependent on the storage form of 25-hydroxyvitamin D₃ (39,40). LL-37 acts as an antibiotic by disrupting the membrane of microbes exhibiting broad-spectrum microbicidal activity against bacteria, fungi, and viruses (10). Direct peptide application and over expression following gene therapy approaches have been precluded because of a number of significant toxicity issues (15–19). Additionally, direct administration of 1,25-hydroxyvitamin D₃ does induce hCAP 18 expression but low concentrations (10^{-7} M 1,25-hydroxyvitamin D₃) generate cytotoxicity and led to the inhibition of cell growth (41–43). Other strategies are therefore needed to improve hCAP 18 expressions and LL-37 productions. A recent study showed that administration of 25-hydroxyvitamin D₃ resulted

in an increase of cathelicidin expression in wounds by activation of CYP27B1 (44). It has been demonstrated that 25-hydroxyvitamin D₃ can enhance innate immunity by inducing a number of cells including keratinocytes, neutrophils, monocytes, macrophages, and epithelial cells which have vitamin D receptor to produce antimicrobial peptides LL-37 (11–14,35–37). In this study, we developed electrospun PLA and PCL fibers as a wound dressing for local sustained delivery of 25-hydroxyvitamin D₃ a circulation form of vitamin D₃ to induce antimicrobial peptide production. Biological effects were demonstrated in plasma-treated and 25-hydroxyvitamin D₃ loaded PCL fibers with increased production of hCAP 18 and LL-37 in HaCat and U937 cells.

Both PLA and PCL fibers are able to encapsulate and deliver 25-hydroxyvitamin D₃ in a sustained manner. The rough surface and ribbon shape of PLA fibers could be due to the high molecular weight and slow diffusion in the solvent of PLA molecules. In contrast, low molecular weight and fast diffusion in the solvent of PCL molecules led to the smooth surface and cylindrical shape of PCL fibers. The *in vitro* release rate of 25-hydroxyvitamin D₃ from PLA and PCL fibers is mainly determined by the rate of polymeric fiber degradation, water penetration, dissolution and diffusion of encapsulated 25-hydroxyvitamin D₃. *In vitro* release results show that 25-hydroxyvitamin D₃ released faster from PLA fibers than from PCL fibers, which could be partly attributed by better hydrophilicity of PLA fibers compared to PCL fibers. Plasma treatment can significantly improve the hydrophilicity and wettability of fibers as water contact angles changed from 150° prior to treatment to 0° after treatment, which could lead to fast water penetration and release rate (Fig. S1). The current study demonstrated that the air plasma treatment enhanced the release rate of 25-hydroxyvitamin D₃ from PLA and PCL fibers. The fiber degradation may have little impact on the release rate of 25-hydroxyvitamin D₃ as both PLA and PCL fibers degraded slowly. Previous studies demonstrated PLA fibers had significant swelling after incubation for 4 weeks (45). The swelling of PLA fibers may enlarge the pore size in fibers and thus enhance the rate of water penetration and diffusion of 25-hydroxyvitamin D₃, eventually resulting in a faster release rate. Therefore, the swelling effect could partially contribute to the faster release rate of 25-hydroxyvitamin D₃ from PLA fibers compared to PCL fibers. The release profiles of 25-hydroxyvitamin D₃ can be further tailored through modulation of degradation rates of fiber materials as the degradation rates of PCL and PLA fibers can be controlled by incorporation of certain enzymes like proteinase K and lipase (46,47). In addition, the improvement of hydrophilicity and wettability of fibers may enhance the absorption of wound exudate. So, it is preferred to treat 25-hydroxyvitamin D₃ loaded PCL and PLA fibers with air plasma. Considering the cost reduction in practical applications, we chose 25-hydroxyvitamin D₃ loaded PCL fibers to conduct the

biological tests because of higher cost of PLA than PCL raw materials.

HaCat cells and U937 cells are human keratinocytes and monocytes, respectively. Both types of cells express CYP27B1 and vitamin D receptor that are essential for the production of hCAP 18 a cathelicidin anti-microbial protein containing the antibacterial peptide LL-37. We demonstrated that HaCat cells incubated with plasma treated and 25-hydroxyvitamin D₃ loaded PCL fibers containing $\sim 5.0 \times 10^{-7}$ M 25-hydroxyvitamin D₃ can express higher level of hCAP 18 and LL-37 compared to the cells administered by 5.0×10^{-6} M 25-hydroxyvitamin D₃ for 5 days with no effects on cytotoxicity (40). Even though the released 25-hydroxyvitamin D₃ from plasma treated and 25-hydroxyvitamin D₃ loaded PCL fibers was much lower than exogenous administered 25-hydroxyvitamin D₃ it was equally effective at LL-37 production indicating a biological advantage of sustained release fiber formulations. Our results also showed that the expression of hCAP 18 and LL-37 of keratinocytes increased after incubation with 5.0×10^{-6} M 25-hydroxyvitamin D₃ from day 1 to 5. In addition, 5.0×10^{-6} M 25-hydroxyvitamin D₃ free drug showed marginal cytotoxic effects on the HaCat cells, which is in accordance with previous studies (40). In contrast, the expression of hCAP 18 and LL-37 of U937 cells after administration of 5.0×10^{-6} M 25-hydroxyvitamin D₃ increased from day 1 to 3 and decreased from day 3 to 5. When incubated with plasma treated and 25-hydroxyvitamin D₃ loaded PCL fibers containing $\sim 5.0 \times 10^{-7}$ M 25-hydroxyvitamin D₃, the expression of hCAP 18 and LL-37 of U937 cells kept increasing from day 1 to 5 with a 10-fold increase in LL-37 production over HaCaT cells (Fig. 6). Most importantly, compared to administration of 5.0×10^{-6} M free drug, U937 cells expressed similar level of hCAP 18 and LL-37 after incubation with plasma treated and 25-hydroxyvitamin D₃ loaded PCL fibers for 3 days, however, the cells expressed significantly higher level of hCAP 18 and LL-37 after incubation with plasma treated and 25-hydroxyvitamin D₃ loaded PCL fibers for 5 days. Additionally, it is revealed that 5.0×10^{-6} M 25-hydroxyvitamin D₃ caused cytotoxicity to U937 after culture for 3 and 5 days as part of monocytes could be killed or the proliferation could be inhibited under such a condition. Cytotoxicity is a concern in this cell line with 5.0×10^{-6} M 25-hydroxyvitamin D₃ altering proliferation within 3 days. In a recent study, 5.0×10^{-6} M or higher concentration of 25-hydroxyvitamin D₃ was demonstrated to be toxic to OKF6-TERT2 and little cytotoxicity was observed when the concentration was lower than 5.0×10^{-7} M, which agrees well with our results in U937 cells (33). So this concentration of 25-hydroxyvitamin D₃ was chosen as a control to test cytotoxicity and should be considered in applications to address surgical site infections. In comparison, the treatment of 5.0×10^{-7} M free drug to HaCat and U937 cells failed to induce production of significant amount of hCAP 18 and LL-37. Plasma treated

and 25-hydroxyvitamin D₃ loaded PCL fibers containing the same amount of 25-hydroxyvitamin D₃ can sustainably induce the production of hCAP 18 and LL-37 in both HaCat and U937 cells, emphasizing the importance of sustained release fiber formulations as novel approach to optimize the biological environment. The results of antibacterial activity indicated that LL-37 in the lysis solutions of U937 cells treated with both 5.0×10^{-6} M 25-hydroxyvitamin D₃ and plasma treated and 25-hydroxyvitamin D₃ loaded PCL fibers for 5 days could kill more bacteria than other treatment groups. EC50 of LL-37 against *Pseudomonas aeruginosa* is around 1.3–3.6 $\mu\text{g/ml}$, and this value against *Staphylococcus aureus* is 1.27 $\mu\text{g/ml}$ (48,49). In this study, there was no infection involved for cultured cells. Therefore, the production level of antimicrobial peptide in this study was relatively low. Even so, we have demonstrated the antimicrobial activity of our system *in vitro*. We will test our delivery system in cultured cells with medium containing supernatant in bacterial culture in our future work. We will also build an *ex vivo* human skin infection model for testing the antibacterial activities of our system in the future work. Our results indicated that the administration of plasma treated and 25-hydroxyvitamin D₃ loaded PCL fibers had no negative effects on the proliferation and simultaneously induced a high-level expression of hCAP 18 and LL-37 in human keratinocytes and monocytes, and LL-37 could kill bacteria to prevent infection, demonstrating a great potential in clinical applications. There is great need for a new approach to develop a post-surgical dressing that reduces the risk of surgical site infections. Current meta-analysis provides no evidence that current products reduce the risk of surgical site infections (50). As only primates and humans have cathelicidin antimicrobial peptide gene, our future work will be focusing on validation of these fiber formulations in a humanized transgenic mouse model or clinical trial testing by comparing systemic administration to localized delivery techniques.

CONCLUSION

25-hydroxyvitamin D₃ loaded PCL and PLA fibers were successfully prepared *via* electrospinning. Plasma treatment improved fiber hydrophilicity and promote the release rate of 25-hydroxyvitamin D₃ from fibers. The 25-hydroxyvitamin D₃ release from PCL and PLA fibers can endure more than 28 days. The released 25-hydroxy vitamin D₃ from electrospun fibers can induce the production of a significantly higher level of hCAP 18/LL-37 than free drugs and LL-37 produced by monocytes could kill bacteria to prevent the occurrence of infection. Plasma treated and 25-hydroxyvitamin D₃ loaded PCL fibers were not exhibiting negative effects on the cell proliferation on human keratinocytes and monocytes. Therefore, the electrospun fibers developed in this study may

be promising as novel dressings for minimizing surgical site infections. These fibers could also be used as coating materials to the implants, devices or catheters for prevention of infections.

ACKNOWLEDGMENTS AND DISCLOSURES

This work was supported partially from startup funds from University of Nebraska Medical Center and National Institute of General Medical Science (NIGMS) grant 2P20 GM103480-06.

REFERENCES

- Humes DJ, Lobo DN. Antisepsis, asepsis and skin preparation. *Surg (Oxf)*. 2009;27(10):441–5.
- Reichman DE, Greenberg JA. Reducing surgical site infections: a review. *Rev Obstet Gynecol*. 2009;2(4):212–21.
- Evans RP, Clyburn TA, Moucha CS, Prokuski L. Surgical site infection prevention and control: an emerging paradigm. *Instr Course Lect*. 2011;60:539–43.
- Awad SS. Adherence to surgical care improvement project measures and post-operative surgical site infections. *Surg Infect*. 2012;13(4):234–7.
- Kohanski MA, Dwyer DJ, Collins JJ. How antibiotics kill bacteria: from targets to networks. *Nat Rev Microbiol*. 2010;8(6):423–35.
- Peleg AY, Seifert H, Paterson DL. *Acinetobacter baumannii*: emergence of a successful pathogen. *Clin Microbiol Rev*. 2008;21(3):538–82.
- Eliopoulos GM, Maragakis LL, Perl TM. *Acinetobacter baumannii*: epidemiology, antimicrobial resistance, and treatment options. *Clin Infect Dis*. 2008;46(8):1254–63.
- Esterly J, Richardson CL, Eltoukhy NS, Qi C, Scheetz MH. Genetic mechanisms of antimicrobial resistance of *acinetobacter baumannii* (Feb). *Ann Pharmacother*. 2011. doi:10.1345/aph.1P084.
- Begum S, Hasan F, Hussain S, Ali SA. Prevalence of multi drug resistant *Acinetobacter baumannii* in the clinical samples from Tertiary Care Hospital in Islamabad, Pakistan. *Pak J Med Sci*. 2013;29(5):1253–8.
- Neville F, Cahuzac M, Kononov O, Ishitsuka Y, Lee KYC, Kuzmenko I, et al. Lipid headgroup discrimination by antimicrobial peptide LL-37: insight into mechanism of action. *Biophys J*. 2006;90(4):1275–87.
- Kemmis CM, Salvador SM, Smith KM, Welsh J. Human mammary epithelial cells express CYP27B1 and are growth inhibited by 25-hydroxyvitamin D-3, the major circulating form of vitamin D-3. *J Nutr*. 2006;136(4):887–92.
- Seifert M, Tilgen W, Reichrath J. Expression of 25-hydroxyvitamin D-1 α -hydroxylase (1 α OHase, CYP27B1) splice variants in HaCaT keratinocytes and other skin cells: modulation by culture conditions and UV-B treatment in vitro. *Anticancer Res*. 2009;29(9):3659–67.
- Viaene L, Evenepoel P, Meijers B, Vanderschueren D, Overbergh L, Mathieu C. Uremia suppresses immune signal-induced CYP27B1 expression in human monocytes. *Am J Nephrol*. 2012;36(6):497–508.
- Pinzone MR, Di Rosa M, Celesia BM, Condorelli F, Malaguarnera M, Madeddu G, et al. LPS and HIV gp120 modulate monocyte/macrophage CYP27B1 and CYP24A1 expression leading to vitamin D consumption and hypovitaminosis D in HIV-infected individuals. *Eur Rev Med Pharmacol Sci*. 2013;17(14):1938–50.
- Suzuki K, Murakami T, Kuwahara-Arai K, Tamura H, Hiramatsu K, Nagaoka I. Human anti-microbial cathelicidin peptide LL-37 suppresses the LPS-induced apoptosis of endothelial cells. *Int Immunol*. 2011;23(3):185–93.
- Henzler Wildman KA, Lee D-K, Ramamoorthy A. Mechanism of lipid bilayer disruption by the human antimicrobial peptide, LL-37. *Biochemistry*. 2003;42(21):6545–58.
- Zhang Z, Cherryholmes G, Shively JE. Neutrophil secondary necrosis is induced by LL-37 derived from cathelicidin. *J Leukoc Biol*. 2008;84(3):780–8.
- Kahlenberg JM, Kaplan MJ. Little peptide, big effects: the role of LL-37 in inflammation and autoimmune disease. *J Immunol*. 2013;191(10):4895–901.
- Steintraesser L, Lam MC, Jacobsen F, Porporato PE, Chereddy KK, Becerikli M, et al. Skin electroporation of a plasmid encoding hCAP-18/LL-37 host defense peptide promotes wound healing. *Mol Ther*. 2014;22(4):734–42.
- Shringirishi M, Prajapati SK, Mahor A, Alok S, Yadav P, Verma A. Nanosponges: a potential nanocarrier for novel drug delivery—a review. *Asian Pac J Trop Dis*. 2014;4(Supplement 2):S519–26.
- Xie J, Wang C-H. Electrospun micro- and nanofibers for sustained delivery of paclitaxel to treat C6 glioma in vitro. *Pharm Res*. 2006;23(8):1817–26.
- Sill TJ, von Recum HA. Electrospinning: applications in drug delivery and tissue engineering. *Biomaterials*. 2008;29(13):1989–2006.
- Choktaweesap N, Arayanarakul K, Duangdao A, Meechaisue C, Supaphol P. Electrospun gelatin fibers: effect of solvent system on morphology and fiber diameters. *Polym J*. 2007;39(6):622–31.
- Hwang SH, Song J, Jung Y, Kweon OY, Song H, Jang J. Electrospun ZnO/TiO₂ composite nanofibers as a bactericidal agent. *Chem Commun*. 2011;47(32):9164–6.
- Maria Spasova DP. Electrospun chitosan-coated fibers of poly(L-lactide) and poly(L-lactide)/poly(ethylene glycol): preparation and characterization. *Macromol Biosci*. 2008;8(2):153–62.
- Chen S, Wang G, Wu T, Zhao X, Liu S, Li G, et al. Silver nanoparticles/ibuprofen-loaded poly(L-lactide) fibrous membrane: anti-infection and anti-adhesion effects. *Int J Mol Sci*. 2014;15(8):14014–25.
- Mohiti-Asli M, Pourdeyhimi B, Lobo EG. Novel, silver-ion-releasing nanofibrous scaffolds exhibit excellent antibacterial efficacy without the use of silver nanoparticles. *Acta Biomater*. 2014;10(5):2096–104.
- Woodruff MA, Huttmacher DW. The return of a forgotten polymer—polycaprolactone in the 21st century. *Prog Polym Sci*. 2010;35(10):1217–56.
- Lin Xiao BW. Poly(Lactic Acid)-based biomaterials: synthesis, modification and applications. In: Dhanjoo NG, editor. *Biomedical science, engineering and technology*. Rijeka: Intech; 2012. p. 247–79.
- Xie J, Willerth SM, Li X, Macewan MR, Rader A, Sakiyama-Elbert SE, et al. The differentiation of embryonic stem cells seeded on electrospun nanofibers into neural lineages. *Biomaterials*. 2009;30(3):354–62.
- Xie J, Liu W, MacEwan MR, Bridgman PC, Xia Y. Neurite outgrowth on electrospun nanofibers with uniaxial alignment: the effects of fiber density, surface coating, and supporting substrate. *ACS Nano*. 2014;8(2):1878–85.
- Jiang J, Xie J, Ma B, Bartlett DE, Xu A, Wang C-H. Mussel-inspired protein-mediated surface functionalization of electrospun nanofibers for pH-responsive drug delivery. *Acta Biomater*. 2014;10(3):1324–32.
- Wang Q, Zhang W, Li H, Apicchio R, Wu W, Lin Y, et al. Effects of 25-hydroxyvitamin D₃ on cathelicidin production and antibacterial function of human oral keratinocytes. *Cell Immunol*. 2013;283(1–2):45–50.

34. Harbarth S, Samore MH, Lichtenberg D, Carmeli Y. Prolonged antibiotic prophylaxis after cardiovascular surgery and its effect on surgical site infections and antimicrobial resistance. *Circulation*. 2000;101(25):2916–21.
35. Liu PT, Stenger S, Li H, Wenzel L, Tan BH, Krutzik SR, et al. Toll-like receptor triggering of a vitamin D-mediated human antimicrobial response. *Science*. 2006;311(5768):1770–3.
36. Selsted ME, Ouellette AJ. Mammalian defensins in the antimicrobial immune response. *Nat Immunol*. 2005;6(6):551–7.
37. Yuk J-M, Shin D-M, Lee H-M, Yang C-S, Jin HS, Kim K-K, et al. Vitamin D3 induces autophagy in human monocytes/macrophages via cathelicidin. *Cell Host Microbe*. 2009;6(3):231–43.
38. Sørensen OE, Follin P, Johnsen AH, Calafat J, Tjabringa GS, Hiemstra PS, et al. Human cathelicidin, hCAP-18, is processed to the antimicrobial peptide LL-37 by extracellular cleavage with proteinase 3. *Blood*. 2001;97(12):3951–9.
39. Stempel N, Neidig A, Nusser M, Geffers R, Vicillard J, Lesouhaitier O, et al. Human host defense peptide LL-37 stimulates virulence factor production and adaptive resistance in *Pseudomonas aeruginosa*. *PLoS One*. 2013;8(12):e82240.
40. Schaubert J, Dorschner RA, Coda AB, Buchau AS, Liu PT, Kiken D, et al. Injury enhances TLR2 function and antimicrobial peptide expression through a vitamin D-dependent mechanism. *J Clin Invest*. 2007;117(3):803–11.
41. Love JF, Tran-Winkler HJ, Wessels MR. Vitamin D and the human antimicrobial peptide LL-37 enhance group A streptococcus resistance to killing by human cells. *Mbio*. 2012;3(5):e00394–12.
42. Gombart AF, Borregaard N, Koeffler HP. Human cathelicidin antimicrobial peptide (CAMP) gene is a direct target of the vitamin D receptor and is strongly up-regulated in myeloid cells by 1,25-dihydroxyvitamin D3. *FASEB J*. 2005;19(9):1067–77.
43. Dixon BM, Barker T, McKinnon T, Cuomo J, Frei B, Borregaard N, et al. Positive correlation between circulating cathelicidin antimicrobial peptide (hCAP18/LL-37) and 25-hydroxyvitamin D levels in healthy adults. *BMC Res Notes*. 2012;5(1):575.
44. Persons KS, Eddy VJ, Chadid S, Deoliveira R, Saha AK, Ray R. Anti-growth effect of 1,25-dihydroxyvitamin D3-3-bromoacetate alone or in combination with 5-amino-imidazole-4-carboxamide-1-beta-4-ribofuranoside in pancreatic cancer cells. *Anticancer Res*. 2010;30(6):1875–80.
45. Ishii D, Ying TH, Mahara A, Murakami S, Yamaoka T, Lee W, et al. In vivo tissue response and degradation behavior of PLLA and stereocomplexed PLA nanofibers. *Biomacromolecules*. 2009;10(2):237–42.
46. Rosa DS, Lopes DR, Calil MR. Thermal properties and enzymatic degradation of blends of poly(ϵ -caprolactone) with starches. *Polym Test*. 2005;24(6):756–61.
47. Masaki K, Kamini NR, Ikeda H, Iefuji H. Cutinase-like enzyme from the yeast *Cryptococcus* sp. strain s-2 hydrolyzes polylactic acid and other biodegradable plastics. *Appl Environ Microbiol*. 2005;71(11):7548–50.
48. Gordon YJ, Huang LC, Romanowski EG, Yates KA, Proske RJ, Mcdermott AM. Human cathelicidin (LL-37), a multifunctional peptide, is expressed by ocular surface epithelia and has potent antibacterial and antiviral activity. *Curr Eyes Res*. 2005;30(5):385–94.
49. Dean SN, Bishop BM, Hoek ML. Natural and synthetic cathelicidin peptides with anti-microbial and anti-biofilm activity against *Staphylococcus aureus*. *BMC Microbiol*. 2011;11(5):114–26.
50. Dumville JC, Gray TA, Walter CJ, Sharp CA, Page T. Dressings for the prevention of surgical site infection. *Cochrane Database Syst Rev*. 2011;6(7), CD003091.